

BadPatches: Backdoor Attacks Against Patch-based Mixture of Experts Architectures

Cedric Chan
Radboud University
Nijmegen, the Netherlands
cedric.chan@ru.nl

Jona te Lintelo
Radboud University
Nijmegen, the Netherlands
jona.telintelo@ru.nl

Stjepan Picek
Radboud University
Nijmegen, the Netherlands
stjepan.picek@ru.nl

ABSTRACT

Deep Neural Networks (DNNs) require large amounts of data and computational power, which limits the usage of these models. Mixture of Experts (MoE) reduces the computational complexity by reducing the total parameters and the amount of training data needed. By leveraging "experts", which are small NNs, the model is able to achieve similar performance with less computational power needed than traditional DNNs. However, these models rely on training data, which introduces backdoor attacks by adversaries. Backdoor attacks embed triggers in the training data to manipulate the model predictions. This study investigates the vulnerability of MoE-based NNs for image classification, a patch-based MoE (pMoE), against backdoor attacks. We examine multiple trigger generation methods and propose a novel trigger application method, BadPatches, that is specifically designed for the patch-level routing mechanism in MoE architectures. BadPatches applies triggers on individual patches rather than on the entire image and achieves better attack success rates than image-level triggers, and achieves successful attacks at poisoning rates as low as 0.01%. Additionally, we investigate fine-pruning as a defense and the relation of patch routing to experts. Results from our experiments show that pMoE is susceptible to backdoor attacks, and we achieve high attack success rates with visible and stealthy triggers. Fine-pruning was able to remove the backdoor only after fine-tuning the backdoored model. Furthermore, we found that there is no strong relation between pixel intensity and patch choosing, and we argue that patch choosing is more likely to be based on feature selection.

KEYWORDS

Backdoor Attack, Mixture of Experts, Image Classification, Convolutional Neural Network, Data Poisoning

1 INTRODUCTION

Deep neural networks (DNNs) have become a popular choice for various tasks in domains such as computer vision [24, 41] or language processing [26]. As computational resources require an increase with the continuously growing size of models [18, 27, 28, 31], new model architectures have been proposed to improve model efficiency. Mixture of Experts (MoE) architectures have emerged as a powerful approach to improve model efficiency [1, 9, 32] by utilizing smaller specialized models called experts, each trained to focus on a different task or subset of data.

The Mixture of Experts architecture was introduced by Jacobs et al. [12] in 1990. Their proposed model consists of expert models and a single gate that combines the expert outputs to generate the final model output. In this model, each input sample is routed to all experts. Shazeer et al. [32] expanded on the idea of combining

smaller expert models to reduce the computational cost of inference with large models. The authors achieve this by reducing the number of parameters used during inference. The authors train multiple smaller experts to focus on different tasks or subsets of data. In addition, a gating network is trained to route input to specific experts. As a result, input is processed using fewer parameters than when the entire model processes it, while maintaining performance. In addition to language models, vision models have also been shown to benefit from the MoE architecture. Chowdhury et al. [6] proposed a patch-level routing mechanism that routes patches of input images to experts for processing. Performing inference on patches of images rather than the entire image reduces sample complexity, computational cost, and requires fewer training samples to achieve performance comparable to a conventional CNN.

As MoE architectures gain traction in research and real-world applications [7, 36], the security considerations of these models [29, 40] are becoming more important. Several works have already shown that non-MoE architectures are vulnerable to malicious attacks [2, 10, 25, 29, 37]. Gu et al. [10] introduced the first backdoor attack, called BadNet. The authors showed that image classification models could misclassify by adding a single pixel or a patch to images and changing the labels to a target label during training. Their attack achieved a high Attack Success Rate (ASR) without a large negative impact on the model's prediction accuracy. Other work [5] proposed blending, or overlaying, an image with the original image to create a trigger that achieves a very high ASR. Expanding on BadNet, multiple works have proposed using stealthy triggers to make the attack less detectable. Liao et al. [22] used a perturbation mask as the trigger that is almost imperceptible to humans when added to images. To create realistic yet stealthy triggers, Nguyen and Tran [25] proposed leveraging altered image characteristics with WaNet. The authors slightly warp the image by shifting a few pixels to create the trigger. Their warped trigger obtained a high ASR in the tested setup and was unsusceptible to state-of-the-art defenses at that time.

However, currently, only one prior work has investigated backdoor attacks against MoE architectures in the text domain. Wang et al. [35] introduce the BadMoE attack and show that an adversary can insert a text trigger that causes, e.g., misclassification in sentiments analysis performed by various MoE architectures. A few works explore the security and privacy considerations of MoE architectures. Puigcerver et al. [29] showed that MoE architectures enjoy better robustness than their dense counterparts. Zhang et al. [40] investigated the adversarial robustness of MoE-CNNs and proposed an adversarial training framework for MoE, AdvMoE, to increase the robustness of MoE architectures. Yona et al. [38]

explored the security and privacy of MoE architectures by showing that an adversary can exploit an MoE, called Mixtral [13], and extract a victim’s prompt. A recent work by Zhang et al. [39] was one of the first to explore adversarial attacks against MoE architectures. The authors showed that Mixtral [13] can be caused to misclassify sentiment analysis via text instructions on multiple levels: word-level, syntax-level, and semantic-level.

In this work, we further explore the vulnerabilities of MoE architectures, specifically a Patch-based Mixture of Experts (pMoE) [6] model, by performing backdoor attacks with different types of triggers. We consider both triggers that are applied on image level and introduce a novel trigger application method, BadPatches, which applies triggers to individual patches rather than entire images. To investigate possible mitigation strategies, we evaluate fine-pruning [23] as a defense against backdoors. Additionally, we analyze the pMoE model’s patch selection to better understand how different triggers influence the router and to which trigger types the pMoE model is more vulnerable. By investigating why certain patches get routed to certain experts, we can examine which factors can be exploited with a trigger to influence the model’s patch selection. This enables more powerful attacks and defenses in the future.¹ Our main contributions are:

- We propose a novel trigger application method called BadPatches, which is specifically designed to generate triggers for the patch-level routing mechanism in MoE architectures. BadPatches outperforms image-level triggers in all conducted experiments.
- To our knowledge, we are the first to investigate the security of MoE-based CNNs with backdoor attacks and show that pMoE-based CNNs are vulnerable to backdoor attacks. We achieve ASRs of up to 100% with visible triggers and a poisoning rate of 2%. With stealthy triggers, we achieve 93.8% ASR with a poisoning rate of 10%.
- We give insight into which image features are important to consider for backdoor attacks and defenses. We show that features such as shape, background, and target object are primary factors in patch selection and that pixel value, contrast intensity, and color have a smaller effect on patch selection.
- We investigate fine-pruning as a defense to mitigate backdoor attacks. We find that pruning neurons is not enough to mitigate the backdoor, with the attack success rate dropping by only ~2%. However, with fine-tuning added, we were able to drop the attack success rate from ~97% to ~2%.

2 PRELIMINARIES

2.1 Mixture of Experts

Mixture of Experts is a type of DNN architecture that uses the output of a single or several experts to produce the final model output. Each expert is a smaller neural network and trained to process only a certain part or type of input through the use of a gating mechanism. The gating mechanism, also called a router, is a network or layer trained separately to determine which expert will process the input. The model’s output is determined by the output of an expert

or by combining the output of multiple experts. Where other DNN architectures use all model parameters, MoE architectures activate only a subset of parameters, which decreases the computational cost for inference. MoE architectures also offer improved scalability and efficiency, making them attractive in Large Language Models (LLMs) [1, 33] and vision models [30]. For instance, DeepSeek leverages MoE to achieve remarkable efficiency and performance [7]. Despite having 671 billion parameters, DeepSeek activates only a small fraction (around 37 billion) for any given task.

2.2 Backdoor Attacks

Poisoning attacks assume that the adversary can access the training data of the ML model. Instead of modifying input at inference time, the adversary injects alterations during the training phase by poisoning the data or the model weights [16]. Poisoning attacks attempt to degrade the model by poisoning the dataset so that the model misclassifies inputs. When poisoning the training data, the adversary can make triggers and add them to inputs so that the model associates the triggers with the chosen target label of the adversary. This is called a backdoor attack, which is a form of poisoning attack. In backdoor attacks, the adversary still attempts to misclassify the inputs, but only when a trigger is present in an input. While most works on backdoor attacks consider computer vision, backdoor attacks also work for other domains such as text [4, 8] and speech recognition [3, 14].

The adversary can choose the target label to misclassify samples as when a trigger is present. However, the adversary can make the backdoor attack more specific by performing a source-specific attack. There, the adversary can not only choose the target label but also add a source label. On the other hand, when random samples are poisoned, all classes in the dataset could contain a trigger, which is commonly called a source-agnostic attack.

3 METHODOLOGY

3.1 Threat Model

3.1.1 Attacker Goal. The attacker’s objective is to cause the target model to misclassify images to the chosen target class at inference time. The backdoor should be stealthy and remain undetected for as long as possible, so the target model should still correctly classify images without the trigger to make the attack more stealthy. Additionally, the triggers should not be easily noticeable, and the number of poisoned images should be low to keep the attack stealthy.

3.1.2 Attacker’s Knowledge & Capabilities. We assume a gray-box setting where the attacker has access to a part of the training data, for which they can alter the labels and the image itself. The attacker does not need to know the model’s architecture or parameters and does not need access to the training procedure.

3.1.3 Real-world Example. Our described threat model can be applied to a real-world scenario where training data is compromised and the adversary has gained access to a part of the dataset. For example, the user uses datasets from untrusted or unknown sources on the internet, obtained through web scraping [17], or datasets that have been formed by crowd-sourcing. In such cases, the datasets may contain malicious inputs that cause the model to behave unexpectedly.

¹Our code is available at <https://github.com/geefmaged/pMoE-backdoor>

3.2 Patch-level Routing in Mixture of Experts

In this work, we use the pMoE architecture designed by Chowdhury et al. [6] to investigate backdoor attacks against MoE architectures in the vision domain. This architecture is a 3-layer Wide Residual Network (WRN) where the last layer of the WRN is replaced by a patch-level MoE (pMoE) layer. A pMoE layer consists of an expert and a router, where each expert is a two-layer CNN with the same architecture. The router in the pMoE architecture directs patches of images, rather than entire images, to an expert. Each training image is divided into l patches of equal size. The routers use the Top-K algorithm to route k patches to each of the n experts. The Top-K patches with the highest activation values after a convolutional layer are routed. A high activation value indicates the patch is influential in the final output of the expert. In the final stage, the outputs from all experts are concatenated, and a softmax activation is applied at the end to produce the final output of the entire model.

Figure 1 illustrates an example pMoE architecture. In this example, images are divided into $l = 16$ patches. The routers use the Top-K algorithm to assign $k = 4$ patches to the $n = 2$ experts. The same patch can be routed to multiple experts. Each expert is trained, and their outputs are concatenated before passing through a dense layer for the final prediction.

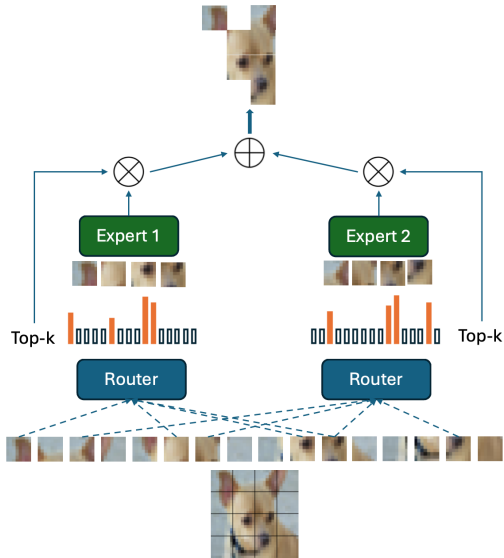


Figure 1: An illustration of the pMoE architecture processing an image. In this specific example, the image is divided into 16 patches, and the router selects 4 patches for each expert.

3.3 Trigger Generation Methods

For our experiments, we selected three different triggers that are common in related work on backdoor attacks to perform our experiments with on the pMoE model. The backdoor attacks we perform are dirty-label attacks, where we change the original labels to the target label ‘0’, corresponding to ‘airplane’. Furthermore, all attacks are performed in a source-agnostic way so that we can evaluate the effects of triggers on a wider range of image features and multiple classes.

3.3.1 Square Trigger. The square trigger we use is based on the trigger used in Badnet [10]. The trigger is a black square with a size of 4×4 pixels and placed in a fixed position in the upper left corner of the image. Our pMoE processes patches of the same 4×4 pixel size, enabling us to track which experts process this trigger with the evaluation method discussed in Section 3.5. Figure 2 shows an example image for the square, blend, and warped trigger applied on the image level.

3.3.2 Blend Trigger. The second trigger we consider is the blend trigger [5]. This trigger generation method involves blending the original image with a trigger image of the same size. In all our experiments, we blend a Hello Kitty image with the original images. The opacity, or weight, of the trigger image can be adjusted based on the blend ratio α . Blending an image can be formally denoted as:

$$x' = (1 - \alpha) \cdot x + \alpha \cdot i,$$

where x is our clean input image, i is the blend image, and α is the blend ratio. We set $\alpha = 0.5$ such that both the input image and the chosen blend image contribute equally to the final backdoored image, x' . This means the poisoned sample will be more distinguishable from clean samples, and we can analyze the effects of a visible trigger present in all patches of an image.

3.3.3 Warped Trigger. In contrast to the previous two trigger methods, we also consider a stealthy backdoor attack using warping in images as a trigger. Warping is an image processing technique that uses geometric transformations to subtly deform images by shifting pixels to different locations. Since these slight pixel movements are hard to perceive, warped images remain visually similar to the originals. Unlike patch-based or blended triggers, which modify pixel colors, warping introduces subtle distortions while preserving the overall appearance, making it a stealthier trigger.

We generate the warping using the method proposed in Nguyen et al. [25]. A vector field is generated to guide the pixel movement in a predefined manner. This process requires two parameters: k , which determines the level of detail in the vector field, and s , which controls the warping strength. Higher values of these parameters result in more pronounced warping, making poisoned images more distinguishable from clean samples. The warping in all our experiments is generated with $k = 2$ and $s = 0.25$ as these settings were shown to create a less noticeable amount of warping but achieve decent ASR in [25]. Unlike the square trigger and blend trigger, we want to focus on the stealthiness of the warped trigger to analyze the effect of stealthy triggers on the pMoE model.

3.3.4 BadPatches. A pMoE architecture divides an input image into patches and, as a result, also divides triggers into patches if they are applied on the entire image, such as the blend and warped trigger. Because of this, the experts in a pMoE architecture will not receive and subsequently process a complete trigger. In the case of smaller triggers, such as the square trigger, it can even be the case that no experts get the patch with the trigger routed, and thus the trigger will not be processed. In this work, we analyze whether triggers can be optimized for the patch-level routing mechanism in MoE architectures, such that we can ensure the trigger is always processed and always processed completely. We propose a novel patch-level trigger application method, called BadPatches. Instead



Figure 2: Examples of a clean image and how the application of different image-level triggers affects the image. The top row shows an image from CIFAR-10, and the bottom row shows an image from GTSRB.

of applying a certain trigger to an entire image, BadPatches applies the trigger to each possible patch in the image. For example, if the input image is 32×32 pixels, and the image is divided into 16×8 patches, then we would apply the same trigger generation method to each of the 16 patches as we normally would on the entire image, practically treating each patch as an image. Applying the Hello Kitty blend trigger with BadPatches requires resizing the trigger image to the size of the patch rather than the input image, but the blend ratio stays equal at $\alpha = 0.5$. By applying a trigger to each possible patch, we ensure the entire trigger is always present in the input to each of the experts and is always processed by each expert in the model, regardless of which patches are routed to the experts. Figure 3 shows examples of poisoned images created with BadPatches.

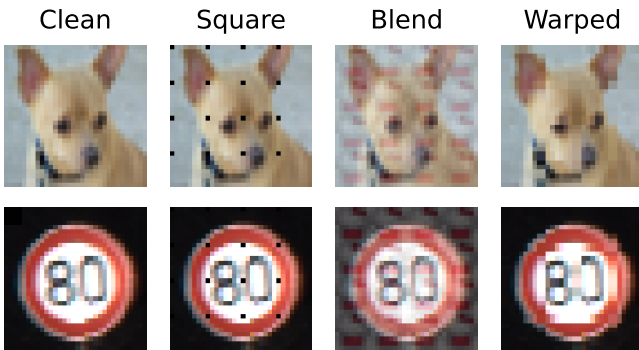


Figure 3: Examples of a clean image and how the application of different BadPatches triggers affect the image. The top row shows an image from CIFAR-10, and the bottom row shows an image from GTSRB.

3.4 Evaluation

To evaluate the performance of the backdoor attacks, we utilize common metrics in the field of poisoning attacks on ML models; Attack Success Rate (ASR), Benign Accuracy (BA), and Clean Accuracy Drop (CAD).

Attack Success Rate (ASR): ASR signals how well the backdoored model predicts the modified test data with the trigger as the chosen target class of the attacker. The modified test data contains test images except the target class, where the trigger is applied to all test images. We calculate the ASR as:

$$\text{ASR} = \frac{\text{\#total predictions of the targeted class}}{\text{\#total predictions}}.$$

Benign Accuracy (BA): BA tells us how well the backdoor model is able to correctly predict the class of the test data without triggers. The BA is calculated as follows:

$$\text{BA} = \frac{\text{\#correct predictions}}{\text{\#total predictions}}.$$

Clean Accuracy Drop (CAD): The CAD indicates the difference in performance between a clean model and a backdoored model on a set of clean images and is represented by the accuracy drop between the two models. The CAD is computed as follows:

$$\text{CAD} = \text{Clean model's accuracy} - \text{Benign accuracy}.$$

3.5 Patch Selection Analysis

The pMoE architecture segments an image into patches, which are then assigned to different experts by routers. To better understand how pMoE distributes these patches, we can visualize which patches are assigned to which expert. By looking at the output of the router in the pMoE layer, we can see which patch indices of an input image are processed by which expert. Using the indices, we create a patch map for every expert showing which patches were processed by that expert. Comparing the maps of different experts and the original image provides insights into the role of features such as shapes and contrast on patch selection. This enables us to better understand which factors are important to consider when choosing an effective type of trigger. Additionally, it allows for model explainability by identifying whether specific experts, or combinations of experts, contribute to misclassification, especially in backdoored models, where certain experts may be responsible for steering images with a trigger toward the target label.

In addition to visualizing the patch selection, we will also look at the pixel values of patches to investigate the influence of pixel value and color. We perform the patch selection analysis and patch value distribution analysis on a wide range of clean and poisoned images from CIFAR-10. We make sure to consider different classes, color distributions, target object size, and contrast where the background is distinct from or similar to the target object.

The pixel values in an image can influence how patches are routed to experts in the pMoE model. This is because the model utilizes the Top-K algorithm, which selects the k highest values. Since the Top-K algorithm selects the highest activation values after a convolutional layer, the pixel intensities within a patch could impact its selection, potentially affecting how patches are distributed among experts based on their pixel values.

Our current method of investigating the influence of color is by making a distribution of patch values for each expert. For each patch, we sum the pixel values, creating a list of patch values for a given image. Theoretically, the maximum patch value occurs when the patch is entirely white. This means that all RGB channels have their highest values, 255 per channel or 1 if normalized, multiplied by the number of pixels per patch, which is 16.

With the patch map we created, we can trace which patches are assigned to which expert and construct a distribution of patch values for each expert. If experts have distinct distributions, where some experts frequently select low-value (darker) patches while others predominantly choose high-value (lighter) patches, it may suggest that the patch assignment to experts is influenced by pixel intensity. This insight could mean that certain experts are biased toward processing patches based on pixel intensity. This information can be exploited by adversaries by developing a specific trigger, based on pixel values, that forces the model to assign poisoned patches to specific experts, leading to controlled misclassification.

3.6 Fine-Pruning Defense

In this work, we consider fine-pruning [23] as a defense because it is commonly used to mitigate the effects of backdoor attacks on non-MoE architectures [11, 19, 21, 23, 25]. Fine-pruning aims to remove the backdoor from the affected model [23] and is a combination of fine-tuning and pruning. The first step is pruning, where some parameter values in the last convolutional layer of every expert are set to 0. The number of parameter values set to 0 is determined by the pruning rate, e.g., a pruning rate of 0.5 indicates that 50% of the parameter values will be set to 0. After pruning, the second step is re-training the model for a number of epochs, also referred to as fine-tuning.

4 EXPERIMENTS

4.1 Data

We evaluate the backdoor attack on two datasets that are used in related work [6, 10, 22, 23, 25]: CIFAR-10 [15] and GTSRB [34]. The CIFAR-10 dataset consists of 50 000 training images and 10 000 test images with 10 classes and input dimensions of $32 \times 32 \times 3$. The GTSRB dataset contains 39 209 training images and 12 630 test images of real-world photos with 43 classes and input dimensions that range from $15 \times 15 \times 3$ to $250 \times 250 \times 3$. Each class has balanced variations in lighting, rotation, background, and scale. We resize all images to $32 \times 32 \times 3$ to be able to use the same model architecture and number of patches as CIFAR-10.

4.2 Baseline models

We consider two baseline models for our experiments to evaluate the effects of our backdoor attack: a clean pMoE model trained on CIFAR-10 and a clean pMoE model trained on GTSRB. For our experiments, we used the pMoE model as described in [6] without modifying the architecture. In all our experiments, we trained our pMoE model with $n = 4$ experts, each expert received $k = 16$ patches, and we divided the images into $l = 64$ patches. These hyperparameter settings were chosen following the results presented [6], which shows these values produce models with good accuracy. We trained and evaluated each baseline model 10 times

and reported the average result to ensure consistency and avoid outliers.

The clean and backdoored models were trained for 25 epochs using the SGD optimizer with a learning rate of 0.1, no decay schedule, and a batch size of 128. Although a learning rate of 0.1 may seem high, we followed the original pMoE implementation’s parameter settings for training as these achieved good results.

Each experiment consists of a dataset, a trigger generation method, and a poisoning rate. We consider the square, blend, and warped trigger described in Section 3, with poisoning rate $\in \{0.1\%, 0.5\%, 2\%, 6\%, 10\%\}$. Each experiment is repeated five times, and we report the average to ensure consistent and reliable results. After each experiment, we apply the evaluation metrics described in Section 3.4 to analyze the results.

To evaluate the effectiveness of BadPatches backdoor attacks, we perform the same experiments as we did for image-level triggers. The training settings and evaluation methods remain the same. However, for BadPatches we report additional results with poisoning rates of 0.05% and 0.01%, because experiments showed that BadPatches would only start to fail at these poisoning rates.

4.3 Fine-Pruning Defense

We evaluate fine-pruning as a defense on a backdoored pMoE model trained with CIFAR-10, a square trigger, and a 2% poisoning rate. Since our primary focus is not on defending pMoE models, we limited the defense experiments to these specific parameters. We perform the defense with a pruning rate of 10%, 20%, and 30% to evaluate how pruning affects the backdoored pMoE model and fine-tune for 5 epochs. Fine-tuning for more epochs could make the defense expensive and is less realistic in our threat model. Additionally, we evaluate the effectiveness of fine-pruning on BadPatches with the same setup and method, and compare it to the image-level fine-pruning results. To ensure reliable results, we run each experiment three times and report the average results.

4.4 Environment Setup

The pMoE implementation is written in Python 3.9.6 using TensorFlow 2.18.0, with Keras handling all model architectures. Our experiments were conducted using Google Colab, utilizing T4 GPUs with 12.7GB system RAM, 15GB GPU RAM, and 112GB disk space. Training times for a single model during our experiments varied from 30 minutes to 45 minutes, depending on the dataset, trigger generation method, and poisoning rate.

5 EXPERIMENTAL RESULTS

5.1 Image-Level Backdoor Attacks

5.1.1 Square Trigger. The results of the image-level backdoor attacks on CIFAR-10 and GTSRB are shown in Tables 1 and 2, respectively. We observe that the square trigger performs well on models trained on CIFAR-10 and GTSRB with a poisoning rate of 0.5% and higher and achieves an ASR of 90.7% up to 99.8%. However, with a very low poisoning rate of 0.1% and lower, the square trigger does not achieve a good result with an ASR of 30.1% and 41.0% on CIFAR-10 and GTSRB, respectively.

We hypothesize two possible reasons for the low ASR when the poisoning rate is 0.1% or lower. First, there are images in the CIFAR-10 and GTSRB datasets that naturally contain dark or black pixels in the upper left corner. When such an image is poisoned with a black square in the upper left corner, it creates a large amount of feature overlap between the trigger and the natural characteristics of the image. Because of this, the visible distinction between trigger and image is minimized. Thus, for these samples, it is difficult for the model to learn to associate the trigger with the target class. Additionally, it is more difficult for the model to learn to associate the trigger with the target class when an image that naturally contains dark or black pixels in the upper left corner is a clean training image. The aim is to have the model associate a single target class with the trigger. When clean images with different classes contain the trigger, it interferes with the model’s training to associate a dark corner only with the target class. The above highlighted issues are exacerbated when the poisoning rate is low. A poisoning rate of 0.1% corresponds to 50 and 39 images in the CIFAR-10 and GTSRB datasets, respectively. When one of the already small number of poisoned images contains natural characteristics that have feature overlap with the trigger, the poisoned dataset gets even smaller. This reduces the opportunities for the model to learn to better distinguish naturally dark pixels in the upper left corner and the trigger, and associate the trigger with the target class.

Our second hypothesis is that, for some images during training, none of the routers select the patch containing the trigger to be evaluated by an expert. If none of the experts process the patch containing the trigger, then for that image, it becomes impossible for the model to learn to associate the trigger with the target class. Again, this issue affects the model more when the poisoning rate becomes lower. With a higher poisoning rate and thus more poisoned samples, it is more likely that patches containing the trigger are at some point selected by a router. In Tables 1 and 2, we indeed observe that a higher poisoning rate increases the attack’s effectiveness. However, for models trained on CIFAR-10 with image-level triggers, the performance drop is also larger when the poisoning rate becomes higher. This can be undesirable as it makes the attack less stealthy.

5.1.2 Blend Trigger. In Tables 1 and 2, we observe that the blend trigger performs well with all poisoning rates and achieves an ASR of 94.7% up to 100%. Compared to the square trigger, the blend trigger achieves a better ASR when the poisoning rate is 0.1%, with 98.3% on CIFAR-10 and 94.7% on GTSRB.

This difference in performance between the square trigger and blend trigger can be attributed to the blend trigger altering every part of the image rather than only the upper left corner. Because of this, the blend trigger is less affected by the two problems hypothesized in Section 5.1. First, if the trigger image is blended with every part of the image, then there is less chance for feature overlap between natural characteristics and the trigger, making it easier for the model to learn to associate the trigger with the target class. Second, if the trigger alters the entire image, then a part of the trigger will always be present in any patch routed to any expert. Thus, making it impossible for the trigger not to be processed, as can be the case with the square trigger on the image level.

However, the trigger altering every part of the image is not enough for a high ASR, as we see with the warped trigger. Although the warped trigger alters all parts of the image, it does not perform well. We expand on these results in Section 5.1.3. The good ASR achieved with the blend trigger can be partially attributed to the blend trigger being less stealthy than the warped trigger, as can be seen in Figure 2.

5.1.3 Warped Trigger. From the results in Tables 1 and 2, we observe that the warped trigger performs worse than the square and blend triggers with an ASR of 0.3% to 93.8%, depending on the poisoning rate. For all poisoning rates and both datasets, the ASR with the warped trigger is lower than with the other trigger types. The warped trigger only achieves a successful result with an ASR higher than 90% when the poisoning rate is 10%, compared to a poisoning rate of 0.5% and 0.1% for the square and blend trigger, respectively.

In Tables 1 and 2, we observe that even though the warped trigger alters every part of the image, it performs significantly worse than the blend trigger. This observation can be attributed to the stealthiness of the trigger. As can be seen in Figure 2, the warped trigger is much less noticeable than the blend trigger. Generally, the ASR becomes lower when triggers become stealthier. This aligns with expectations based on previous work [20, 42] on stealthy triggers that show higher poisoning rates are needed to achieve an ASR comparable to non-stealthy triggers.

The warped trigger with poisoning rates of 0.5% to 6.0% achieves a higher ASR for models trained on GTSRB than models trained on CIFAR-10. A possible reason for these results is that warping effects are more noticeable in GTSRB images than in CIFAR-10 images, as seen in Figure 2. As the warping effect visibly changes more parts of the GTSRB image, the trigger is less stealthy than in most CIFAR-10 images, but increases ASR. Additionally, dividing up the image into patches is less disruptive to the trigger when the warping effect is stronger. As more patches with stronger warping get routed to experts. Resulting in the model being able to better learn to associate the warping with the target class.

5.2 BadPatches Backdoor Attacks

The results for BadPatches are shown in Tables 1 and 2. We observe that BadPatches performs well on all datasets and achieves an ASR higher than 90%, except with the warped trigger and poisoning rates of 0.5% and lower. The BadPatches backdoor attacks start to fail with a poisoning rate of 0.01% for the square trigger and blend trigger, corresponding to only 5 and 3 poisoned samples in the training set for CIFAR-10 and GTSRB, respectively. However, at 0.01% poisoning rate, BadPatches still results in a successful attack with the blend trigger on GTSRB, achieving an ASR of 90.3%.

Comparing the results between image-level triggers and BadPatches in Tables 1 and 2, it can be seen that BadPatches achieves a higher ASR in all experiments and a slightly better benign accuracy in some experiments than the backdoor attacks with image-level triggers. We observe that BadPatches performs better with triggers and poisoning rates that do not perform well on image-level. Notably, BadPatches achieves successful results at lower poisoning rates than image-level triggers. When the poisoning rate is 0.1%, the image-level square trigger achieves an ASR of 30.1% and 41.0%

Table 1: Experimental results backdoor attacks with different types of triggers on pMoE models trained on CIFAR-10.

| Method | Poison Rate | Square | | | Blend | | | Warped | | |
|-------------|-------------|----------------|---------------|------------------|----------------|---------------|------------------|----------------|---------------|------------------|
| | | ASR \uparrow | BA \uparrow | CAD \downarrow | ASR \uparrow | BA \uparrow | CAD \downarrow | ASR \uparrow | BA \uparrow | CAD \downarrow |
| Image-Level | 0.1 | 30.1 | 83.8 | 1.2 | 98.3 | 83.5 | 1.5 | 3.5 | 83.9 | 1.1 |
| | 0.5 | 90.7 | 83.5 | 1.5 | 99.6 | 83.3 | 1.7 | 8.2 | 83.8 | 1.2 |
| | 2.0 | 96.6 | 83.2 | 1.8 | 99.9 | 83.5 | 1.5 | 24.5 | 83.0 | 2.0 |
| | 6.0 | 97.4 | 83.1 | 1.9 | 99.9 | 83.2 | 1.8 | 54.9 | 82.1 | 2.9 |
| | 10.0 | 99.1 | 82.7 | 2.3 | 100.0 | 82.1 | 2.9 | 93.8 | 82.9 | 2.1 |
| BadPatches | 0.01 | 72.7 | 83.8 | 1.2 | 78.9 | 83.6 | 1.4 | 5.3 | 83.3 | 1.7 |
| | 0.05 | 96.6 | 84.3 | 0.7 | 99.9 | 83.9 | 1.1 | 11.8 | 83.5 | 1.5 |
| | 0.1 | 95.1 | 83.4 | 1.6 | 99.9 | 84.0 | 1.0 | 19.1 | 83.9 | 1.1 |
| | 0.5 | 99.8 | 83.6 | 1.4 | 99.9 | 83.4 | 1.6 | 74.9 | 83.6 | 1.4 |
| | 2.0 | 100.0 | 83.3 | 1.7 | 100.0 | 82.6 | 2.4 | 95.6 | 83.8 | 1.2 |
| | 6.0 | 100.0 | 83.8 | 1.2 | 100.0 | 83.5 | 1.5 | 99.1 | 82.1 | 2.9 |
| | 10.0 | 100.0 | 82.5 | 2.5 | 100.0 | 83.3 | 1.7 | 99.8 | 82.3 | 2.7 |

Table 2: Experimental results backdoor attacks with different types of triggers on pMoE models trained on GTSRB.

| Method | Poison Rate | Square | | | Blend | | | Warped | | |
|-------------|-------------|----------------|---------------|------------------|----------------|---------------|------------------|----------------|---------------|------------------|
| | | ASR \uparrow | BA \uparrow | CAD \downarrow | ASR \uparrow | BA \uparrow | CAD \downarrow | ASR \uparrow | BA \uparrow | CAD \downarrow |
| Image-Level | 0.1 | 41.0 | 97.8 | 0.2 | 94.7 | 97.1 | 0.9 | 0.3 | 97.0 | 1.0 |
| | 0.5 | 98.2 | 97.5 | 0.5 | 99.2 | 97.2 | 0.8 | 20.1 | 97.2 | 0.8 |
| | 2.0 | 99.7 | 97.4 | 0.6 | 100.0 | 97.0 | 1.0 | 45.5 | 97.1 | 0.9 |
| | 6.0 | 99.8 | 97.5 | 0.5 | 100.0 | 97.0 | 1.0 | 77.4 | 97.0 | 1.0 |
| | 10.0 | 99.8 | 96.9 | 1.1 | 100.0 | 96.5 | 1.5 | 91.6 | 96.6 | 1.4 |
| BadPatches | 0.01 | 63.0 | 97.6 | 0.4 | 90.3 | 97.3 | 0.7 | 0.0 | 97.1 | 0.9 |
| | 0.05 | 97.6 | 97.3 | 0.7 | 96.0 | 97.5 | 0.5 | 0.3 | 97.6 | 0.4 |
| | 0.1 | 99.8 | 97.3 | 0.7 | 98.3 | 97.4 | 0.6 | 6.1 | 97.2 | 0.8 |
| | 0.5 | 99.9 | 97.4 | 0.6 | 99.8 | 97.3 | 0.7 | 37.5 | 97.5 | 0.5 |
| | 2.0 | 100.0 | 97.3 | 0.7 | 100.0 | 97.5 | 0.5 | 90.4 | 97.3 | 0.7 |
| | 6.0 | 100.0 | 96.8 | 1.2 | 100.0 | 97.4 | 0.6 | 97.9 | 97.4 | 0.6 |
| | 10.0 | 100.0 | 97.7 | 0.3 | 100.0 | 97.5 | 0.5 | 99.8 | 97.2 | 0.8 |

on CIFAR-10 and GTSRB, respectively. Only at poisoning rates of 0.5% is the attack successful. However, BadPatches with the square trigger still achieves ASRs of 96.6% and 97.6% with a poisoning rate of 0.05%, and only starts to fail when the poisoning rate is 0.01%. A similar observation is made for the warped trigger. The image-level warped only achieves a good ASR of 93.8% and 91.6% at 10.0% poisoning rate. Whereas BadPatches achieves a good ASR of 95.6% and 90.4% with 2.0% poisoning rate, only starting to fail at 0.5% poisoning rate. These results show that BadPatches is able to achieve successful attacks with lower poisoning rates than image-level triggers and performs better than image-level triggers for all triggers and poisoning rates.

Additionally, the results in Tables 1 and 2 show there is no large negative impact on the accuracy of the poisoned model. Comparing the BA and CAD between all experiments, there is no more than 0.7% BA drop difference between BadPatches and the image-level

triggers. Meaning there is no significant trade-off between the increased ASR and the accuracy of the model for using BadPatches instead of image-level triggers.

We hypothesize that the improved ASR results are primarily because the complete trigger is applied to every patch in that image. As mentioned in Sections 3.3.4 and 5.1, there are two drawbacks to applying image-level triggers to images when processed by the patch routing mechanism. First, the trigger might be present in a few patches or no patches at all that are routed to experts. Second, triggers that are applied to the entire image will be divided up during the patch selection, resulting in an irregular trigger pattern being processed by the experts. The triggers applied using BadPatches do not suffer from these two drawbacks. Consider the square trigger; if a black square is applied to every possible patch routed to any expert, then we can enforce that every expert in all training steps learns to associate the trigger with the target class. In

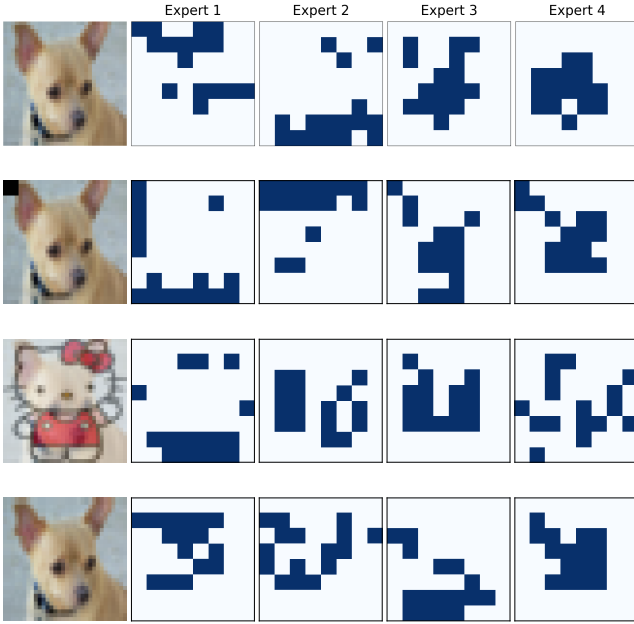


Figure 4: Patch selection for the same image in models backdoored with image-level triggers. Every row shows which patches each of the four experts processes.

the case of the blend and warped trigger, the entire trigger is applied to each patch. This ensures the complete trigger is processed by any expert and eliminates irregular processing of only parts of the trigger.

5.3 Patch Selection Analysis

5.3.1 Effects of Triggers on Patch Selection. Figures 4 and 5 show how the clean model routes clean images and how poisoned models route the patches for their respective triggers. We observe that the application of triggers alters patch selection for all experts. In the case of the image-level square trigger in Figure 4, all experts get the top left patch containing the black square routed. However, the patch routing for the BadPatches square trigger shows none of the experts get the top left patch containing the black square routed. This shows that training the model on a poisoned dataset affects the patch selection of the model in such a way that ensures the trigger gets processed by the model.

5.3.2 Clean Model Patch Selection. Figure 6 displays which patches of an image are routed to which expert for the pMoE model trained for 25 epochs. The first two rows display a plane and a cat image from CIFAR-10, and the last two rows show images from the GTSRB dataset. In Figure 6, we see that each expert gets routed a different set of patches with varying degrees of overlap. Some experts may receive more patches containing pixels affected by the trigger than others. This means not every expert is equally influenced by triggers. For some triggers present in only certain patches of the image, e.g., the square trigger, it can happen that only one expert will process the trigger and still cause misclassification.

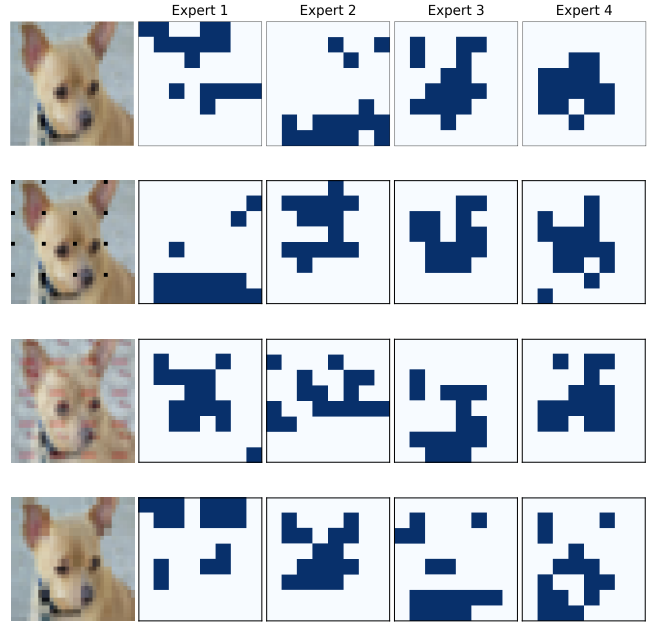


Figure 5: Patch selection for the same image in models backdoored with BadPatches triggers. Every row shows which patches each of the four experts processes.

Generally, we observe that for a specific class, some experts learn to focus on parts of the background, while others learn to focus on the target object. This behavior can be seen in the example images for GTSRB. For both GTSRB example images, experts 1 and 2 focus on the central shape of the sign, while experts 3 and 4 often focus on the outline and edges of objects in images. Similar behavior is observed for some of the CIFAR-10 images. In the example image of the cat, we see that only expert 1 has a strong focus on the central object, i.e., the face of the cat. This behavior indicates that the shape of objects is an important factor in patch selection. Triggers that visibly affect the shape of objects in images will have a large influence on these experts.

Additionally, we observe in our experiments that the same expert can learn to focus on the background or target object depending on the class rather than having a fixed specialization for the location or shape of objects in images. In the examples of Figure 6, it can be seen that expert 4 learns to focus on large parts of the background for the cat, whilst in the plane image it focuses on the target object. Similar observations are made for other classes and images, indicating that another important factor in patch selection is whether the expert specializes in the target object or background for that class. This means that if a trigger only affects the target object, the trigger will only influence certain experts.

In Figure 7, we show the distributions of the average pixel value of the patches per expert. In the distributions for the cat image in Figure 7a, we observe that experts 1, 2, and 3 show peaks in frequency for certain average patch value bins. For example, expert 1 has a high frequency of patches with an average patch value of around 13. Additionally, there is a strong clustering of average

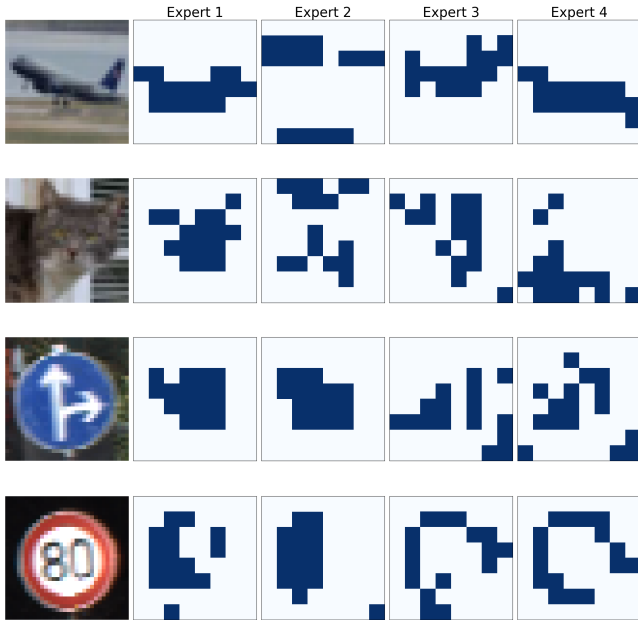


Figure 6: Patch selection for each expert of the clean pMoE model. The first column shows the input images, and subsequent columns show which expert was assigned which patches. The first two rows show CIFAR-10 images, and the last two rows show GTSRB images.

values. For example, expert 1 has 13 out of 16 patches with an average patch value between 10 and 20. However, from Figures 7a and 7b we also see that the values for which there are peaks and clusters in the distributions of experts are random and differ per class and even per image. Moreover, in Figure 6 it can be seen that an expert does not only choose patches that have the same color, i.e., pixel values. This indicates that routers likely use pixel values to discern the shape of objects in images. This results in clusters around certain values that dominate an object in the image, but no strong bias for a patch selection pattern based on a certain color.

5.4 Fine-Pruning Defense

In Table 3, we display the results of the fine-pruning defense performed on both an image-level and BadPatches backdoored pMoE model trained on CIFAR-10 with the square trigger and 2% poisoning rate. For the image-level backdoor, it can be seen that the fine-pruning defense successfully mitigates the effects of the backdoor attack and reduces the ASR from 96.6% to as low as 1.9%. For the BadPatches backdoor attack, fine-pruning also effectively mitigates the effects of the backdoor attack and reduces the ASR from 100.0% to as low as 26.8%. However, fine-pruning as a defense is not as effective on pMoE models backdoored with BadPatches as it is with image-level triggers.

We observe in Table 3 that different pruning rates result in nearly the same ASR reduction and that most ASR reduction occurs after fine-tuning. This contradicts expectations based on the fine-pruning defense proposed in [23], where pruning is intended to remove

Table 3: Results of the fine-pruning defense on pMoE trained on the CIFAR-10 dataset, backdoored with a square trigger and 2% poisoning rate. Reported results are the average over three runs. A higher ASR indicates the defense is less effective in mitigating the backdoor’s effects.

| Pruning Rate | | Image-Level | | BadPatches | |
|--------------|-------------------|---------------|----------------|---------------|----------------|
| | | BA \uparrow | ASR \uparrow | BA \uparrow | ASR \uparrow |
| | Before Defense | 83.2 | 96.6 | 83.3 | 100.0 |
| 10% | After Pruning | 80.1 | 94.2 | 81.0 | 100.0 |
| | After Fine-Tuning | 83.5 | 2.1 | 82.2 | 23.1 |
| 20% | After Pruning | 78.9 | 95.2 | 82.0 | 99.9 |
| | After Fine-Tuning | 83.6 | 1.9 | 80.8 | 26.8 |
| 30% | After Pruning | 72.2 | 95.3 | 80.9 | 99.9 |
| | After Fine-Tuning | 83.5 | 2.2 | 82.8 | 29.7 |

backdoor neurons, while fine-tuning is mainly used to restore the classification accuracy on clean samples. We hypothesize this behavior is because fine-pruning only prunes the last convolutional layer in the model. It is possible that the backdoor is present in a different layer or multiple layers of the pMoE model. In this case, pruning would have no effect on the backdoor because we prune only the last convolutional layer.

In addition, the class prediction accuracy drops substantially when the pruning rate increases. With a 30% pruning rate, the clean accuracy dropped from 85.2% to 72.2% after pruning, and from 84.9% to 80.1% with a 10% pruning rate. The failure to remove the backdoor and the reduction in performance show that pruning itself is not an effective defense and that fine-tuning, or retraining, the model removes the backdoor.

Figure 8 shows the effect of fine-pruning on patch selection. Before fine-pruning, three out of four experts would process the square trigger patch, indicating it to be an influential patch for classification. However, after fine-pruning, there is only one out of four experts who process the patch containing the square trigger, meaning the trigger patch has much less influence on the final classification. This change in routing provides a visual explanation for the backdoor attack’s reduced effectiveness after fine-pruning.

6 CONCLUSIONS AND FUTURE WORK

In this work, we investigate the vulnerability of an MoE-based CNNs, pMoE, against backdoor attacks. We have demonstrated that pMoE architectures are susceptible to backdoor attacks in various settings by using three different trigger generation methods. Additionally, we have introduced a novel trigger application method, called BadPatches, that is specifically designed for the patch-level routing mechanism in the pMoE architecture. We have shown that BadPatches achieves better ASRs than image-level triggers without sacrificing accuracy on clean images. Even with very low poisoning rates of 0.01%, an adversary can perform a successful attack and achieve a high ASR by utilizing a visible trigger. For both visible and stealthy triggers, the CAD increases only marginally with an increased poisoning rate, indicating that a higher poisoning rate does not affect the performance of the model significantly. This

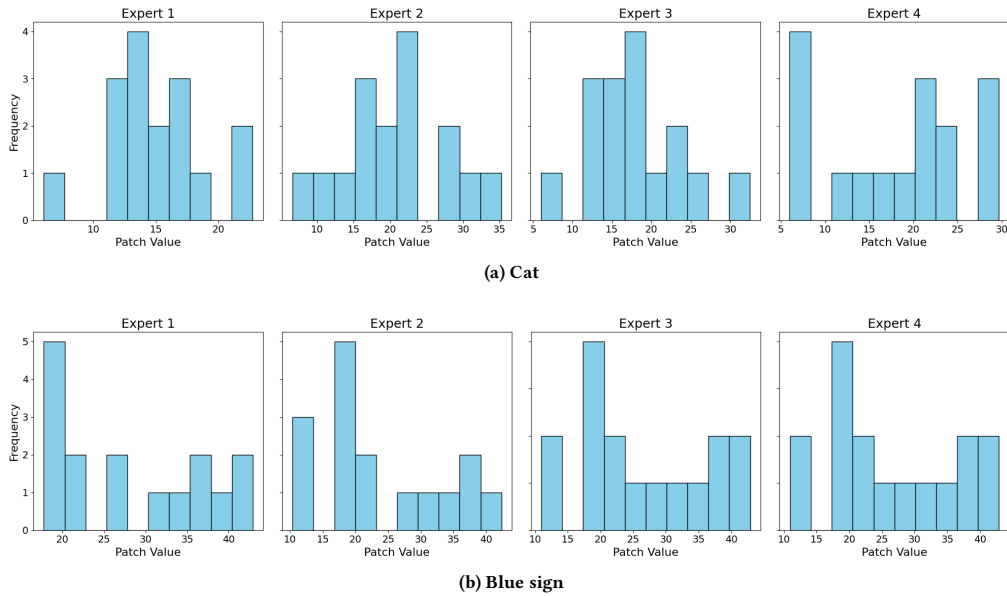


Figure 7: Patch value distributions of images from Figure 6. On the x-axis are the average pixel values of the patches that were routed to that expert. On the y-axis are the frequencies of occurrence for the average pixel values.

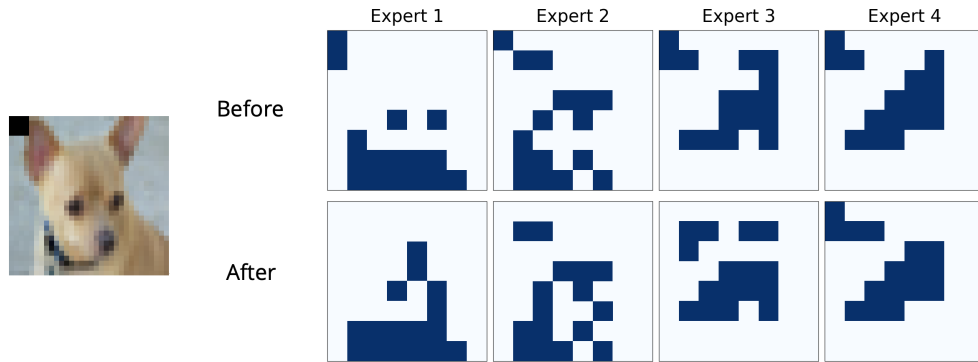


Figure 8: CIFAR-10 image of a dog poisoned with the square trigger and the corresponding patch selection for the four experts before and after fine-pruning. The top row shows the patch selection before fine-pruning, and the bottom row shows the patch selection after fine-pruning.

makes pMoE architectures extra vulnerable to backdoor attacks, as the attack is more stealthy when the accuracy on clean images is not affected by the backdoor training. In this work, we also investigated fine-pruning as a defense against backdoor attacks for pMoE architectures. We found that fine-pruning is able to remove the backdoor successfully and reduce ASR from 96.6% to 1.9% for image-level backdoors, whilst sacrificing 1.4% prediction accuracy on clean images. However, the majority of the backdoor removal happens in the fine-tuning stage. The pruning stage of the defense does little to reduce ASR and has a large negative impact on the prediction accuracy. Showing that fine-tuning is an effective way to mitigate the effects of backdoor attacks on pMoE architectures,

but pruning is not. Future works include investigating backdoor attacks on different MoE architectures, such as V-MoE, and datasets with different properties, such as larger images. Moreover, the performance of BadPatches can be investigated on other patch-based MoEs than CNNs, such as vision transformers. Additionally, as this work only considers MoE in the vision domain, an interesting direction is investigating the vulnerabilities of MoE architectures in the text domain against backdoor attacks or other adversarial attacks.

REFERENCES

- [1] Artetxe, M., Bhosale, S., Goyal, N., Mihaylov, T., Ott, M., Shleifer, S., Lin, X.V., Du, J., Iyer, S., et al., R.P.: Efficient large scale language modeling with mixtures of experts. arXiv preprint **arXiv:2112.10684** (2021), <https://arxiv.org/abs/2112.10684>
- [2] Bai, J., Gao, K., Gong, D., Xia, S.T., Li, Z., Liu, W.: Hardly perceptible trojan attack against neural networks with bit flips. arXiv preprint **arXiv:2207.13417** (2022), <https://arxiv.org/abs/2207.13417>
- [3] Cai, H., Zhang, P., Dong, H., Xiao, Y., Koffas, S., Li, Y.: Towards stealthy backdoor attacks against speech recognition via elements of sound. arXiv preprint **arXiv:2307.08208** (2023), <https://arxiv.org/abs/2307.08208>
- [4] Chen, X., Salem, A., Chen, D., Backes, M., Ma, S., Shen, Q., Wu, Z., Zhang, Y.: Badnl: Backdoor attacks against nlp models with semantic-preserving improvements. In: Annual Computer Security Applications Conference. p. 554–569. ACSAC '21, ACM (Dec 2021). <https://doi.org/10.1145/3485832.3485837>, <http://dx.doi.org/10.1145/3485832.3485837>
- [5] Chen, X., Liu, C., Li, B., Lu, K., Song, D.: Targeted backdoor attacks on deep learning systems using data poisoning. arXiv preprint **arXiv:1712.05526** (2017), <http://arxiv.org/abs/1712.05526>
- [6] Chowdhury, M.N.R., Zhang, S., Wang, M., Liu, S., Chen, P.Y.: Patch-level routing in mixture-of-experts is provably sample-efficient for convolutional neural networks. arXiv preprint **arXiv:2306.04073** (2023), <https://arxiv.org/abs/2306.04073>
- [7] DeepSeek-AI, Liu, A., Feng, B., Xue, B., Wang, B., Wu, B., Lu, C., Zhao, C., Deng, C., Zhang, C., Ruan, C., Dai, D., Guo, D., Yang, D., Chen, D., et al., D.J.: Deepseek-v3 technical report. arXiv preprint **arXiv:2412.19437** (2025), <https://arxiv.org/abs/2412.19437>
- [8] Du, W., Yuan, T., Zhao, H., Liu, G.: Nws: Natural textual backdoor attacks via word substitution. In: ICASSP 2024 - 2024 IEEE International Conference on Acoustics, Speech and Signal Processing (ICASSP). pp. 4680–4684 (2024). <https://doi.org/10.1109/ICASSP48485.2024.10447968>
- [9] Fedus, W., Zoph, B., Shazeer, N.: Switch transformers: Scaling to trillion parameter models with simple and efficient sparsity. arXiv preprint **arXiv:2101.03961** (2021), <https://arxiv.org/abs/2101.03961>
- [10] Gu, T., Dolan-Gavitt, B., Garg, S.: Badnets: Identifying vulnerabilities in the machine learning model supply chain. arXiv preprint **arXiv:1805.12185** (2017), <http://arxiv.org/abs/1708.06733>
- [11] Hong, S., Carlini, N., Kurakin, A.: Handcrafted backdoors in deep neural networks. In: Koyejo, S., Mohamed, S., Agarwal, A., Belgrave, D., Cho, K., Oh, A. (eds.) Advances in Neural Information Processing Systems. vol. 35, pp. 8068–8080. Curran Associates, Inc. (2022). https://proceedings.neurips.cc/paper_files/paper/2022/file/3538a22cd3ceb8f009c62b9e535c29f-Paper-Conference.pdf
- [12] Jacobs, R.A., Jordan, M.I., Nowlan, S.J., Hinton, G.E.: Adaptive mixtures of local experts. *Neural Computation* **3**(1), 79–87 (1991). <https://doi.org/10.1162/neco.1991.3.1.79>
- [13] Jiang, A.Q., Sablayrolles, A., Roux, A., Mensch, A., Savary, B., Bamford, C., Chaplot, D.S., de las Casas, D., Hanna, E.B., et al., F.B.: Mixtral of experts. arXiv preprint **arXiv:2401.04088** (2024), <https://arxiv.org/abs/2401.04088>
- [14] Koffas, S., Xu, J., Conti, M., Picek, S.: Can you hear it? backdoor attacks via ultrasonic triggers. In: Proceedings of the 2022 ACM Workshop on Wireless Security and Machine Learning. p. 57–62. WiseML '22, Association for Computing Machinery, New York, NY, USA (2022). <https://doi.org/10.1145/3522783.3529523>
- [15] Krizhevsky, A., Hinton, G.: Learning multiple layers of features from tiny images. Tech. Rep. 0, University of Toronto, Toronto, Ontario (2009), <https://www.cs.toronto.edu/~kriz/learning-features-2009-TR.pdf>
- [16] Kurita, K., Michel, P., Neubig, G.: Weight poisoning attacks on pre-trained models. arXiv preprint **arXiv:2004.06660** (2020), <https://arxiv.org/abs/2004.06660>
- [17] Kuznetsova, A., Rom, H., Alldrin, N., Uijlings, J.R.R., Krasin, I., Pont-Tuset, J., Kamali, S., Popov, S., Mallocci, M., Duerig, T., Ferrari, V.: The open images dataset V4: unified image classification, object detection, and visual relationship detection at scale. arXiv preprint **arXiv:1811.00982** (2018), <http://arxiv.org/abs/1811.00982>
- [18] Larochelle, H., Bengio, Y., Louradour, J., Lamblin, P.: Exploring strategies for training deep neural networks. *Journal of Machine Learning Research* **10**(1), 1–40 (2009), <http://jmlr.org/papers/v10/larochelle09a.html>
- [19] Li, Y., Lyu, X., Koren, N., Lyu, L., Li, B., Ma, X.: Anti-backdoor learning: Training clean models on poisoned data. *Advances in Neural Information Processing Systems* **34**, 14900–14912 (2021)
- [20] Li, Y., Li, Y., Wu, B., Li, L., He, R., Lyu, S.: Backdoor attack with sample-specific triggers. arXiv preprint **arXiv:2012.03816** (2020), <https://arxiv.org/abs/2012.03816>
- [21] Li, Y., Li, Y., Wu, B., Li, L., He, R., Lyu, S.: Invisible backdoor attack with sample-specific triggers. In: Proceedings of the IEEE/CVF international conference on computer vision. pp. 16463–16472 (2021)
- [22] Liao, C., Zhong, H., Squicciarini, A.C., Zhu, S., Miller, D.J.: Backdoor embedding in convolutional neural network models via invisible perturbation. arXiv preprint **arXiv:1808.10307** (2018), <http://arxiv.org/abs/1808.10307>
- [23] Liu, K., Dolan-Gavitt, B., Garg, S.: Fine-pruning: Defending against backdooring attacks on deep neural networks. arXiv preprint **arXiv:1805.12185** (2018), <http://arxiv.org/abs/1805.12185>
- [24] Minaee, S., Boykov, Y., Porikli, F., Plaza, A., Kehtarnavaz, N., Terzopoulos, D.: Image segmentation using deep learning: A survey. arXiv preprint **arXiv:2001.05566** (2020), <https://arxiv.org/abs/2001.05566>
- [25] Nguyen, T.A., Tran, A.T.: Wanet - imperceptible warping-based backdoor attack. arXiv preprint **arXiv:2102.10369** (2021), <https://arxiv.org/abs/2102.10369>
- [26] Otter, D.W., Medina, J.R., Kalita, J.K.: A survey of the usages of deep learning for natural language processing. *IEEE Transactions on Neural Networks and Learning Systems* **32**(2), 604–624 (2021). <https://doi.org/10.1109/TNNLS.2020.2979670>
- [27] Patterson, D., Gilbert, J.M., Gruteser, M., Robles, E., Sekar, K., Wei, Y., Zhu, T.: Energy and emissions of machine learning on smartphones vs. the cloud. *Commun. ACM* **67**(2), 86–97 (jan 2024). <https://doi.org/10.1145/3624719>
- [28] Patterson, D., Gonzalez, J., Le, Q., Liang, C., Munguia, L.M., Rothchild, D., So, D., Texier, M., Dean, J.: Carbon emissions and large neural network training (2021)
- [29] Puigcerver, J., Jenatton, R., Riquelme, C., Awasthi, P., Bhojanapalli, S.: On the adversarial robustness of mixture of experts. arXiv preprint **arXiv:2210.10253** (2022), <https://arxiv.org/abs/2210.10253>
- [30] Riquelme, C., Puigcerver, J., Mustafa, B., Neumann, M., Jenatton, R., Pinto, A.S., Keyes, D., Houlsby, N.: Scaling vision with sparse mixture of experts. arXiv preprint **arXiv:2106.05974** (2021), <https://arxiv.org/abs/2106.05974>
- [31] Samsi, S., Zhao, D., McDonald, J., Li, B., Michaleas, A., Jones, M., Bergeron, W., Kepner, J., Tiwari, D., Gadepally, V.: From words to watts: Benchmarking the energy costs of large language model inference (2023)
- [32] Shazeer, N., Mirhoseini, A., Maziarz, K., Davis, A., Le, Q.V., Hinton, G.E., Dean, J.: Outrageously large neural networks: The sparsely-gated mixture-of-experts layer. arXiv preprint **arXiv:1701.06538** (2017), <http://arxiv.org/abs/1701.06538>
- [33] Shen, S., Hou, L., Zhou, Y., Du, N., Longpre, S., Wei, J., Chung, H.W., Zoph, B., et al., W.F.: Mixture-of-experts meets instruction tuning: a winning combination for large language models. arXiv preprint **arXiv:2305.14705** (2023), <https://arxiv.org/abs/2305.14705>
- [34] Stalkamp, J., Schlipf, M., Salmen, J., Igel, C.: The german traffic sign recognition benchmark: A multi-class classification competition. In: The 2011 International Joint Conference on Neural Networks. pp. 1453–1460 (2011). <https://doi.org/10.1109/IJCNN.2011.6033395>
- [35] Wang, Q., Pang, Q., Lin, X., Wang, S., Wu, D.: Badmoe: Backdooring mixture-of-experts llms via optimizing routing triggers and infecting dormant experts (2025), <https://arxiv.org/abs/2504.18598>
- [36] Xue, F., Zheng, Z., Fu, Y., Ni, J., Zheng, Z., Zhou, W., You, Y.: Openmoe: An early effort on open mixture-of-experts language models. arXiv preprint **arXiv:2402.01739** (2024), <https://arxiv.org/abs/2402.01739>
- [37] Xue, M., Ni, S., Wu, Y., Zhang, Y., Wang, J., Liu, W.: Imperceptible and multi-channel backdoor attack against deep neural networks. arXiv preprint **arXiv:2201.13164** (2022), <https://arxiv.org/abs/2201.13164>
- [38] Yona, I., Shumailov, I., Hayes, J., Carlini, N.: Stealing user prompts from mixture of experts (2024), <https://arxiv.org/abs/2410.22884>
- [39] Zhang, R., Li, H., Wen, R., Jiang, W., Zhang, Y., Backes, M., Shen, Y., Zhang, Y.: Instruction backdoor attacks against customized llms. arXiv preprint **arXiv:2402.09179** (2024), <https://arxiv.org/abs/2402.09179>
- [40] Zhang, Y., Cai, R., Chen, T., Zhang, G., Zhang, H., Chen, P.Y., Chang, S., Wang, Z., Liu, S.: Robust mixture-of-expert training for convolutional neural networks. arXiv preprint **arXiv:2308.10110** (2023), <https://arxiv.org/abs/2308.10110>
- [41] Zhao, Z., Zheng, P., Xu, S., Wu, X.: Object detection with deep learning: A review. arXiv preprint **arXiv:1807.05511** (2018), <http://arxiv.org/abs/1807.05511>
- [42] Zhong, N., Qian, Z., Zhang, X.: Imperceptible backdoor attack: From input space to feature representation. arXiv preprint **arXiv:2205.03190** (2022), <https://arxiv.org/abs/2205.03190>